Kinetics and Catalysis, Vol. 41, No. 6, 2000, pp. 729–736. Translated from Kinetika i Kataliz, Vol. 41, No. 6, 2000, pp. 805–813.
Original Russian Text Copyright © 2000 by Krestinin.

On the Kinetics of Heterogeneous Acetylene Pyrolysis

A. V. Krestinin

Institute of Problems of Chemical Physics, Russian Academy of Sciences, Chernogolvka, Moscow oblast, 142432 Russia

Received April 29, 1999

Abstract—The independent experimental data on the variation of the rate of carbon film formation on the hot cylinder surface in an acetylene–argon flow are theoretically analyzed. The quantitative model uses the detailed mechanism of the gas-phase pyrolysis of acetylene and takes into account both thermal conductivity and diffusion of the gaseous components in the boundary layer. An increase in the rate of the heterogeneous thermal decomposition of acetylene experimentally observed at high temperatures cannot be described within the framework of the pyrocarbon formation mechanism that accounts for the contribution of the products of the partial gas-phase pyrolysis of acetylene. The experimental data are quantitatively described using the model developed earlier for the growth of soot particles. The quantitative macrokinetics of the heterogeneous growth of the carbon film is determined assuming that the above description correctly reflects an experimental increase in the rate of the heterogeneous reaction.

INTRODUCTION

Acetylene is the main product of hydrocarbon pyrolysis at temperatures above ~1273 K. Therefore, its heterogeneous decomposition requires extensive investigation. Tesner [1] published a comprehensive review of the available data on pyrocarbon formation from gaseous hydrocarbons. The rate of pyrocarbon formation from acetylene at temperatures below 1273 K was repeatedly measured and found to be proportional to the acetylene concentration with a rate constant of $1.7 \times 10^{-6} \times \exp(-33[\text{kcal/mol}]/RT)$ g cm^{-2} s^{-1} Pa^{-1} [2, 3]. The kinetic measurements of the heterogeneous pyrolysis above 1273 K are hampered by the contribution of the products of the gas-phase decomposition of acetylene to pyrocarbon formation. Al'tshuler [4, 5] measured the rate of carbon film formation from gaseous acetylene at 1400–2400 K using a thin cylindrical conductor heated by electric current in a gas flow. The apparent rate constant was $2.5 \times 10^{-6} \times \exp(-30[\text{kcal/mol}]/RT)$ g cm^{-2} s^{-1} Pa^{-1} up to 1700 K, which agrees well with that measured in [2, 3] under different experimental conditions. However, the experimental rate of pyrocarbon formation abruptly increases above 1700 K, as expressed by the first-order equation with the rate constant $1.5\exp(-76[\text{kcal/mol}]/RT)$ g cm^{-2} s^{-1} Pa^{-1} [4, 5]. Figure 1 presents the Arrhenius plot of the rate constant for carbon film formation. The rate constant values (in cm/s) were obtained by processing the initial data using the equation k^{het} (cm/s) = $((RT/\Delta m)k^{\text{het}}$ (g cm^{-2} s^{-1} Pa^{-1}), where R (Pa cm^3 K^{-1} mol^{-1}) is the universal gas constant and $\Delta m = 24$ (g/mol) is a gain in the carbon film weight during the pyrolysis of 1 mol of acetylene. An increase in the rate of carbon film formation was explained by the contribution of the products of acetylene gas-phase decomposition, although it remaines unclear what decomposition products play a key role in this process. Kiefer and von Drasek recently carried out an extensive kinetic study of the gas-phase pyrolysis of acetylene [6]. Their data enable a comprehensive numerical analysis of the problem, including calculating the rate of pyrocarbon formation taking into account the gas-phase pyrolysis of acetylene in the boundary layer and determining the contribution of the products of this reaction to carbon film growth. This was one of the goals of our present study.

The data obtained in [4, 5] also suggest that an experimental increase in the rate of carbon film formation is related to the formation of soot particles. The soot growth rate during hydrocarbon pyrolysis is 2–3 orders of magnitude higher than that of pyrocarbon formation in the gaseous medium of the same composition [7]. This phenomenon has not been explained so far. Obviously, the mechanism of carbon film formation, including the heterogeneous decomposition of gaseous hydrocarbons to pyrocarbon at the hot surface, changes to some other mechanism at high temperatures. In this case, an approach developed earlier [8–12] to describe the kinetics of soot particlegrowth should also be applicable to the growth of the carbon film in the above experiments without special changes. Therefore, the second goal of this study was to check the polyine model of soot formation under experimental conditions that were not taken into account when building this model.

MODEL OF CARBON FILM FORMATION FOR EXPERIMENTAL CONDITIONS OF [4, 5]

When gas flows around a cylinder, a thin boundary layer is formed near the cylinder surface, within which the gas flow rate ranges from zero on the cylinder surface to the value corresponding to the stream running on the outer surface of the boundary layer. The boundary layer thickness is estimated as $\delta = 1.2\ d/(\text{Re})^{0.5}$, where d is the cylinder diameter, $\text{Re} = Ud/\nu$ is the Rey-

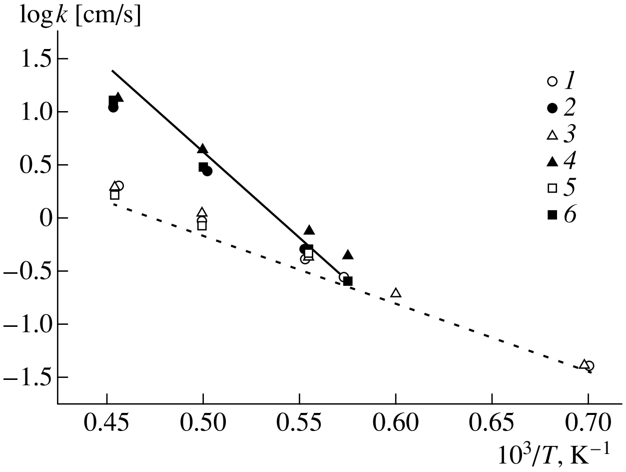

Fig. 1. The Arrhenius plot of the apparent rate constant for the heterogeneous pyrolysis of acetylene. Experiment: (dotted line) $k_1 = 1.25 \times 10^3 \exp(-30\ [\text{kcal/mol}]/RT)$ cm/s [4, 5] and (solid line) $k_2 = 7.5 \times 10^8 \exp(-76\ [\text{kcal/mol}]/RT)$ cm/s. Calculation: the reduced rate of the formation ($w/[C_2H_2]$, cm/s) of (*1*, *3*, *5*) pyrocarbon and (*2*, *4*, *6*) coke for the (*1*, *2*) 10% C_2H_2/Ar mixture and $\delta = 0.037$ cm, (*3*, *4*) 10% C_2H_2/Ar and $\delta = 0.045$ cm, and (*5*, *6*) 20% C_2H_2/Ar and $\delta = 0.022$ cm.

nolds number, U is the gas flow rate, and ν is the kinematic gas viscosity [13]. Taking into account the parameters used in the experiments of [4, 5] (the gas flow rate $U = 1.5 \times 10^3$ cm/s, the conductor diameter $d = 0.03$ cm, and the kinematic gas viscosity $\nu = 1.5\ \text{cm}^2/\text{s}$), the boundary layer thickness δ is estimated to be ~0.01–0.02 cm. Neglecting the convective transfer within the boundary layer, the following equations and boundary conditions can be used to quantitatively describe carbon film growth:

$$-y^{-k}\frac{\partial}{\partial y}y^k J_i + r_i = 0,\quad J_i\big|_{y = d/2} = r_i^{\text{het}},$$

$$a_i\big|_{y = d/2+\delta} = a_{0,i},\quad i = 1, \dots, n, \tag{1}$$

$$-y^{-k}\frac{\partial}{\partial y}y^k J_T + q = 0,\quad T\big|_{y = d/2} = T_s,\quad T\big|_{y = d/2+\delta} = T_0.$$

Here, y is the coordinate along the boundary layer thickness perpendicular to the surface of a solid; $k = 0$ for the flat boundary layer and $k = 1$ for the cylindrical one; a_i is the relative weight concentration of chemical gaseous component (n is the number of components); T is the gas temperature; r_i and q are the sources of chemical components and heat due to the gas-phase reactions, respectively; J_i and J_T are the gaseous component and heat flows due to diffusion and thermal conductivity, respectively; T_0 and $a_{0,i}$ are the temperatures and concentrations of the gaseous components in the oncoming stream, respectively; T_s is the temperature of the hot surface at which the carbon film is formed; and r_i^{het} are the sources (sinks) of the chemical gaseous components in heterogeneous reactions. The boundary layer thickness slowly increases near the cylinder surface along the current lines from the point of the flow stop [13]. Convective transfer within the boundary layer is negligible. These two facts together make the gas composition near the cylinder surface dependent on the coordinate along the boundary layer. Let us assume that these corrections are negligible compared to the effects used in the description and let us eliminate them from set (1) of the equations. This set of equations also neglects the formation and growth of soot particles in the gas phase and their contribution to carbon film formation. The inclusion of the equations of the polyine model of soot formation [10–12] into set (1) indicated that this process can be neglected under the experimental conditions of [4, 5] up to 2000–2200 K. This can be attributed to the fact that the nucleation zone shifts from the hot wall inside the boundary layer with the maximum concentrations of higher polyines as was shown by the calculations. Despite a higher temperature, their concentrations near the surface are lower because of the high rate of heterogeneous decay (Table 1). Growing soot particles are extruded from the boundary layer by thermophoresis, and their contribution to the kinetics of the bulk pyrolysis of acetylene near the walls remains insignificant. The contribution of soot formation becomes noticeable only at a rather high temperature or in the case of a thick boundary layer, that is, under conditions that were beyond the scope of this work.

The scheme of the reactions of the gas-phase pyrolysis of acetylene taken from [6] and slightly corrected includes nearly a hundred reversible chemical reactions involving 27 different chemical gaseous components. The description of the chemical growth of the carbon film on the surface is similar to that of the polyine model of soot formation for the growth of soot particles [8–12], and the rate constants for elementary steps are the same. A brief description of the method is presented below, and details can be found elsewhere [10–12].

The polyine model of soot formation implies that gaseous polyines $C_{2n}H_2$ ($n = 2, 3, \dots$) can form a polymer during the radical–chain polymerization on the surface. It is also assumed that the radical–chain polymerization occurs only if the rate of formation of the surface polymer layer is higher than that of carburization of the resulting polymer. Therefore, the polyine model includes two different mechanisms of carbon film formation on the surface of a solid (or aerosol species) in a hydrocarbon atmosphere. One is pyrocarbon formation when the rate of polymer growth w_{gr} is lower than the rate of its carburization w_{carb}. The kinetics of this process is studied in detail by Tesner and Borodina [1–3], who measured the rate constants for the heterogeneous pyrolysis of a number of hydrocarbons. When calculating the rate of pyrocarbon formation in this work, I took into account the contribution of the main products of the bulk pyrolysis of acetylene, including

Table 1. Scheme of the heterogeneous reactions of pyrocarbon (PC) formation and their rate constants

No.	Reaction[a]	$k^{het} = A\exp(-E/RT)$, cm/s		
		A, cm/s	E, kcal/mol	Reference for the A and E values
1	$C_2H_2 \longrightarrow$ PC	1250	30	[5]
2	$C_4H_2 \longrightarrow$ PC	10^b	10^b	This work, estimates
3	$C_6H_2 \longrightarrow$ PC	40^c	5	″
4	$C_8H_2 \longrightarrow$ PC	100^c	0	″
5	$C_{10}H_2 \longrightarrow$ PC	200^c	0	″
6	$C_4H_4 \longrightarrow$ PC	1000	27.5	[1]
7	$H^\bullet \longrightarrow$ decay	200	0	This work, estimates
8	$C_{2n}H^\bullet \longrightarrow$ PC, $n = 1, 2, ...$	4000^d	0	″
9	$C_2H_3^\bullet \longrightarrow$ PC	50	0	″
10	$C_4H_3^\bullet \longrightarrow$ PC	50	0	″
11	$C_{2n}H_3^\bullet \longrightarrow$ PC, $n = 3, 4, ...$	2000^d	0	″

[a] The rate of carbon film formation by the $x_i \longrightarrow$ PC reaction with the rate constant k_i^{het} (cm/s): w (g cm^{-2} s^{-1}) = $\Delta m_i k_i^{het}[x_i]$, where Δm_i (g/mol) is the increment in the weight of the condensed phase during the pyrolysis of the 1 mol of the gaseous x_i species and $[x_i]$ (mol/cm^3) is the concentration of the x_i species.

[b] $A = 4$ cm/s, $E = 14.8$ kcal/mol [1].

[c] These rate constants are not available; they are apparently overestimated.

[d] The efficiency of radical decay is most likely overestimated (see the text).

radicals. Table 1 presents these reactions with the rate constants used in the calculations. For many reactions listed in Table 1, the kinetic parameters are currently unknown and cannot be theoretically estimated with sufficient accuracy. The choice of the apparent kinetic parameters for certain reactions is discussed below. The general idea was to arrive at an upper estimate of the carbon film growth rate based on the mechanism of pyrocarbon formation.

Another mechanism implies the formation of a polymeric material (coke), which occurs when the rate of polymer growth w_{gr} is higher than that of carburization w_{carb}. It is assumed that, under the conditions of coke formation, the surface of a polymer layer is covered with the C–H groups that produce local radical sites where the C–H bond is cleaved to eliminate a hydrogen atom. The polymeric layer grows mostly via heterogeneous reactions on these radical sites.

The model also implies that polyines $C_{2n}H_2$, ($n = 2, 3, \ldots$) favor branching in the chain polymerization as soon as a complex of several polyine molecules is formed on the surface radical site. Additional radical sites in this case are formed by the cyclization reaction, which inevitably occurs in this polyine complex. The assumption of branching in the chain polymerization of polyines is necessary to explain the fact that certain radicals (soot nuclei) irreversibly grow during the formation of new species. Within the framework of the polyine model, new soot particles are formed only when the condition of polyine vapor supersaturation is met:

$$w_{br} > w_{term} + w_{carb}. \quad (2)$$

Here, w_{br} is the rate of branching of the surface radical sites (mol cm^{-2} s^{-1}), $w_{term} + w_{carb}$ (mol cm^{-2} s^{-1}) is the rate of their decay by both the heterogeneous reactions involving gaseous molecules and radicals (w_{term}) and the carburization of the polymeric material (w_{carb}). During the whole nucleation period when condition (2) is met, the occupation of the surface of the growing soot particles with radical sites is maximal. Therefore, coke formation at this stage can be called “rapid polymerization.” Haynes and Wagner [14] and Minutolo *et al.* [15] suggested a certain process that forms the basis for the growth of soot particles during their formation, which is often referred to as rapid polymerization. Many researchers are surprised by the tremendously high experimental rates of soot particle growth resulting in the formation of aerosol species with diameters of several hundreds of angstroms for several milliseconds in the flames. By analogy with the condensation of the supersaturated vapor of simple substances, condition (2) can be considered as a condition for polyine vapor supersaturation. Indeed, if it is met, the probability of branching for any surface site for growth is higher than that the probability of its decay, the gaseous radicals (nuclei) that can produce a polyine complex become

Table 2. Heterogeneous reactions of polymer growth

Reaction type[a]	Rate constant $k^{het} = A\exp(-E/RT)$, cm/s		Prototype reaction (k is the rate constant, $cm^3\ mol^{-1}\ s^{-1}$)
	A, cm/s	E, kcal/mol	
Generation of radical sites			
$C{-}H + H^\bullet \longrightarrow C^\bullet + H_2$[b]	1400	16	$PhH + H \longrightarrow Ph + H_2$, ($k = 2.5 \times 10^{14}\exp(-16[kcal/mol]/RT)$, [21])
Decay of radical sites			
$C^\bullet + H_2 \longrightarrow C{-}H + H^\bullet$	80	12	$Ph + H_2 \longrightarrow PhH + H^\bullet$, ($k = 2.5 \times 10^{13}\exp(-11[kcal/mol]/RT)$, [21])
$C^\bullet + C_2H_2 \longrightarrow C{-}C_2H + H^\bullet$	150	12	$Ph + C_2H_2 \longrightarrow PhC_2H + H^\bullet$, ($k = 4.0 \times 10^{13}\exp(-11.6[kcal/mol]/RT)$, [22])
$C^\bullet + ArH \longrightarrow C{-}Ar + H^\bullet$[c]	9	4	$Ph + PhH \longrightarrow PhPh + H^\bullet$, ($k = 4.0 \times 10^{11}\exp(-4[kcal/mol]/RT)$, [22])
$C^\bullet + H^\bullet \longrightarrow C{-}H$	200	0	$Ph + H^\bullet \longrightarrow PhH$, ($k = 10^{13}$, [23])
$C^\bullet + R^\bullet \longrightarrow C{-}R$[c]	200	0	$Ph + C_2^\bullet H \longrightarrow PhC_2H$, ($k = 10^{13}$, [23])
Polyine polymerization on radical sites			
$C^\bullet + C_{2n}H_2 \longrightarrow C{-}PY^\bullet$[b] $n = 2, 3, \ldots$	200	0	$C_2^\bullet H_3 + C_2H_2 \longrightarrow C_4H_5$ ($k = 10^{13}$, [23])
Branching of radical sites[d]			
$C{-}PY^\bullet + C_4H_2 \longrightarrow 1.2C^\bullet$	600	0	–
$C{-}PY^\bullet + C_{2n}H_2 \longrightarrow 2C^\bullet$, $n = 3, \ldots$	600	0	–

[a] See Note (a) to Table 1.

[b] $C^\bullet$ is the surface radical site, $C{-}PY^\bullet$ is the surface radical site with the polyine molecule attached to it.

[c] Ar is the aryl radical; $R^\bullet$ is the hydrocarbon radical.

[d] In the branching reactions, the coefficients on the right side denote the average number of the radical sites formed upon the rearrangement of the polyine complex structure.

the sites for polyine polymerization and irreversibly grow into polymeric globules, which are the initial forms of soot particles.

In terms of the polyine model, the kinetics of carbon film formation at the stage of polymer formation can approximately be described by the following set of equations [11, 12], the steady-state solution to which is obtained at infinity:

$$\begin{aligned}(N_A\Delta)^{-1}\frac{d\alpha}{dt} &= (1-\alpha)w_{gen} \\ &\quad - \alpha(w_{term}+w_{carb}) + \alpha_1 w_{pol}(n_{br}-1), \\ (N_A\Delta)^{-1}\frac{d\alpha_1}{dt} &= (\alpha-\alpha_1)w_{pol} \\ &\quad - \alpha_1(w_{term}+w_{carb}+w_{pol}).\end{aligned} \tag{3}$$

Here, α ($0 \le \alpha$) is the surface coverage by radical sites; α_1 ($\alpha_1 \le 1$) is the surface coverage by radical sites with one attached polyine molecule; w_{geb} is the rate of radical site generation at the inert polymer surface by H-atom abstraction from the C–H group, w_{term} is the rate of their decay in the heterogeneous reactions involving gaseous molecules and radicals, and w_{carb} ($mol\ cm^{-2}\ s^{-1}$) is the rate of their decay by polymeric material carburization; w_{pol} ($mol\ cm^{-2}\ s^{-1}$) is the rate of polyine addition to radical sites; $(n_{br} - 1) > 0$ is the degree of branching of the sites for growth (the average number of additional radical sites generated upon the restructuring of a polyine complex); Δ is the surface area occupied by one surface radical site, $\sim 10^{-15}\ cm^2$ [16]; and N_A is the Avogadro number. The approximate expression for the branching rate w_{br}, which is true under steady-state conditions at $w_{term} + w_{carb} \gg w_{gen}$ is

$$w_{br} = w_{pol}^2 (n_{br}-1)/(w_{term}+w_{carb}+2w_{pol}). \tag{4}$$

The rate constants for the heterogeneous reactions at the stage of polymer formation given in Table 2 are estimated using the model based on the approach suggested by Howard [16]. This approach implies that the surface radical site and the gaseous phenyl radical exhibit the same chemical activity. Taking this into account, the rate of the heterogeneous reaction can be determined by the number of collisions of gaseous species with the surface radical sites multiplied by the coefficient calculated from the available kinetic data for the gas-phase analogous reaction. This coefficient is equal to the ratio of the rate constant for the analogous reaction to the number of binary collisions between gaseous reactants involved in the reaction. Within the framework of this approach, the expression for the rate of the heterogeneous reaction takes the form [10]:

$$k^{\text{het}} = 0.25(\mu/m_{\text{X}})^{0.5}k^{+}/(N_{\text{A}}\pi R^{2}_{\text{C}^{\bullet}}), \tag{5}$$

where k^{het} is the rate constant for the heterogeneous reaction (cm/s); k^{+} (cm^3 mol^{-1} s^{-1}) is the rate constant for the gas-phase prototype reaction between the phenyl radical Ph with a molecule (radical) X; m_{X} and μ are the weight of the X species and the reduced weight of the Ph–X pair, respectively; and $R_{\text{C}^{\bullet}}$ (cm) is the collision radius for the surface radical site $\text{C}^{\bullet}$. Although this approach is not ideal, it allows for estimating the unknown rate constants for heterogeneous reactions in a consistent way so that their main error can be represented by a factor that is almost independent of temperature and reaction type. This unknown scaling factor takes into account the difference in the chemical activities of the phenyl radical and the surface radical site in reaction with the same gaseous species.

The rate of the decay of the surface sites by the carburization of the polymeric material can be estimated as $w_{\text{carb}} = k_{\text{carb}}/(N_{\text{A}}\Delta)$, where k_{carb} is the apparent first-order rate constant for carburization. The k_{carb} value, measured for the soot particles formed in the ethylene flame [17], is $1.8 \times 10^6 \times \exp(-27\ [\text{kcal/mol}]/RT)$ s^{-1}. In general, the carburization rate depends on the chemical composition of the gas phase surrounding a growing particle. For example, the addition of benzene vapors to diacetylene allows one to decrease the rate of carburization of the soot particle material and thus obtain samples of translucent soot particles, the microphotographs of which are shown in [18]. This provides direct evidence for the polymeric nature of the soot material at an early stage of particle formation. At the stage of coke formation, the rate of carbon film formation can be expressed as $w_{\text{gr}} = \alpha m_{\text{pol}} w_{\text{pol}}$, where m_{pol} is the average weight of 1 mol of polyines involved in polymerization.

Note that, despite the fact that the above polyine model is presented in chemical terms, it cannot be considered as a strict physicochemical variant of the mechanism of soot formation. Nevertheless, it is still useful as a quantitative kinetic model, and its practical application was confirmed by the perfect agreement between the calculated and experimental data for all main parameters of soot formation during hydrocarbon pyrolysis, such as the induction period, the concentration of the soot particles, and the soot yield. The calculations were performed for 900–2000 K and for different hydrocarbons: methane, acetylene, ethylene, benzene, diacetylene, and naphthalene [12].

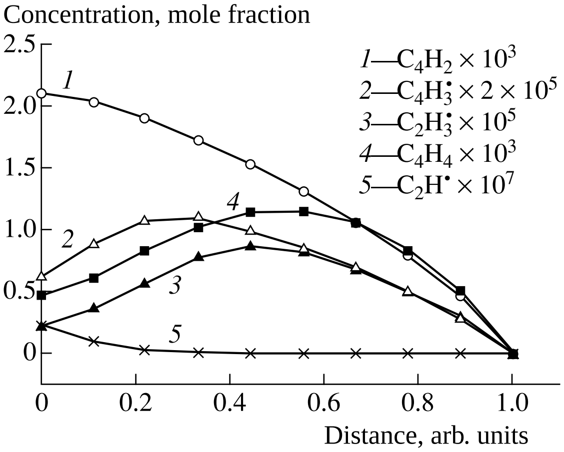

Fig. 2. Concentration profiles for the products of the gas phase pyrolysis of acetylene in the boundary layer. The calculation was performed for the surface temperature of 1740 K, the acetylene concentration in the flow of 10%, and the boundary layer thickness $\delta = 0.037$ cm. The H_2 concentration virtually coincides with the profile of the diacetylene concentration. The ratio of the distance from the carbon film surface to the δ value is plotted along the x axis.

RESULTS AND DISCUSSION

Figure 1 compares the Arrhenius plots of the rate constant for carbon film formation [4, 5] and the reduced rate (with the apparent first-order rate constant) $w/[C_2H_2]$ calculated according to the above model, where the rate w is expressed in mol cm^{-2} s^{-1}. The diffusion flows in set (1) of the equations were calculated in the binary diffusion approximation. The diffusion coefficients in argon for polyines and other species of linear structure with the carbon skeleton C_{2n} were estimated by the equation $D_{C_{2n}} = D_{C_2H_2}(1/n)$. This relationship follows from the expression for the binary diffusion coefficient $D \sim \langle v \rangle/(\sigma^* N)$, where $\langle v \rangle$ is the average relative rate of the species, $\sigma^* \sim 2n$ is the cross-section of the collision of the inert gas atom with the linear carbon cluster species [19, 20], and N is the concentration in the mixture 1/cm^3). Calculations presented in Fig. 1 neglect the temperature dependence of the boundary layer thickness. For the 10% C_2H_2/Ar mixture, the value of $\delta = 0.037$ cm was chosen in such a way that the transition from pyrocarbon to polymer formation occurred at 1740–1800 K, as was observed in the experiment. This boundary layer thickness seems slightly overestimated as compared to the estimates for the experimental conditions of [4, 5]. However, to

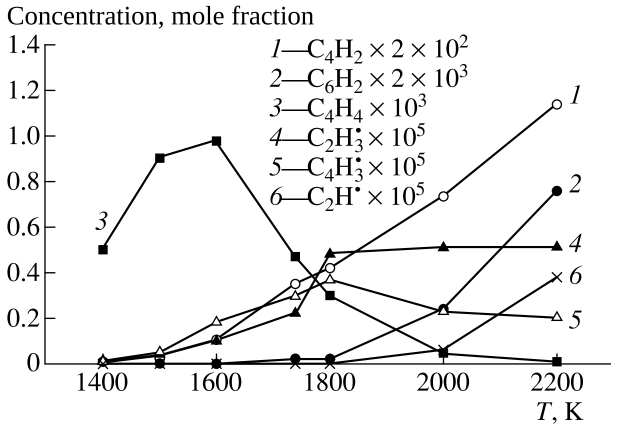

Fig. 3. Concentrations of the products of the gas-phase pyrolysis of acetylene near the surface as a function of the surface temperature. The calculation was performed for the acetylene concentration in the flow of 10% and the boundary layer thickens $\delta = 0.037$ cm.

obtain the appropriate agreement with the experiment, δ was set to 0.022 cm in the calculations with the acetylene concentration of 20%, which was also used in the cited papers (Fig. 1). Note that the apparent thickness of the boundary layer can be measured in the experiments as the thickness of the smoked region surrounding the heated cylindrical conductor and, thus, the chosen numerical values can be checked. As follows from the slope of the Arrhenius curves in Fig. 1, the activation energy for polymer formation obtained from the calculation data assuming that the δ value is temperature independent is slightly lower than the experimental one. However, $\delta \sim T$, and this correction provides a better agreement between the experimental and calculated activation energies.

Figure 2 presents the profiles of the concentrations of the stable products of the bulk pyrolysis of acetylene as functions of the boundary layer thickness (which are higher than 10^{-4} mole fraction) and the concentrations of several hydrocarbon radicals that contribute significantly to the surface growth of the carbon film. Among the pyrolysis products not shown in Fig. 2, note ethylene (C_2H_4) with a concentration of $\sim 0.8 \times 10^{-4}$ mole fraction near the surface, triacetylene (C_6H_2) ($\sim 10^{-5}$ mole fraction), and hexene-3-diene-1,5 (HC≡C–CH≡CH–C≡CH) ($\sim 0.5 \times 10^{-4}$ mole fraction). The calculations show that diacetylene and the $C_2H_3^{\bullet}$ and $C_4H_3^{\bullet}$ radicals (with the rate constants for decay listed in Table 1), in addition to acetylene make the main contribution to the rate of carbon film formation under the conditions of pyrocarbon formation at ~1700 K.

Above 1700 K, only polyines, such as diacetylene and triacetylene, make a noticeable contribution to the process in addition to acetylene. The rate constants for the heterogeneous pyrolysis of polyines are unknown, and the values listed in Table 1 most likely exceed their contribution to pyrocarbon formation. Nevertheless, even in this case, the calculated rate of carbon film growth during pyrocarbon formation remains much lower than the experimental one.

At temperatures up to 2200 K, the $C_2H^{\bullet}$ radical does not affect carbon film growth, although the rate constant for its decay is close to the maximal value (Table 1). This estimate for the rate constant follows from the fact that the rate of the heterogeneous reaction should be lower than the rate of the gaseous species flow to the surface (or the average number of collisions with a unit surface per unit time) equal to $\sim 1/4 \langle v \rangle [X]$ mol cm^{-2} s^{-1}, where $\langle v \rangle$ (cm/s) is the average thermal rate of the gaseous reactant species and [X] (mol/cm^3) is the reactant concentration. For C_2 hydrocarbons, $1/4\langle v \rangle \cong 2 \times 10^4$ cm/s at $T = 1500$ K. Thus, the efficiency of the decay of the $C_2H_3^{\bullet}$ and $C_4H_3^{\bullet}$ radicals (the number of efficient collisions with the surface divided by the overall number of collisions) was set equal to $\sim(2\text{–}5) \times 10^{-3}$ in Table 1. It may appear that an increase in the rate constants for the heterogeneous reactions for these radicals by 1–1.5 orders of magnitude results in an agreement between the experimental and calculated results and that the calculated rate of carbon film growth during pyrocarbon formation coincides with the experimental one. Figure 2 shows that the maximum concentration of these radicals is shifted from the surface into the bulk of the boundary layer. This indicates that the rate of their heterogeneous decay is diffusion-controlled. Therefore, an increase in the rate constants only slightly affects the contribution of the radicals to carbon film formation. I deliberately set a rather low rate constant for the heterogeneous decay of the H radical in Table 1. This leads to overestimating the conversion of the gas-phase pyrolysis of acetylene in the boundary layer. However, the products of the bulk pyrolysis under these conditions are insufficient to obtain the observed rate of carbon film growth by the mechanism of pyrocarbon formation.

Figure 3 illustrates how the concentrations of the products of acetylene pyrolysis in the bulk near the hot surface change with the surface temperature. Above 1800 K, the $C_2H_3^{\bullet}$ and $C_4H_3^{\bullet}$ concentrations remain unchanged on heating. This provides further evidence for the fact that an experimental apparent activation energy for carbon film formation of 76 kcal/mol cannot be obtained at high temperatures by an increase in the contribution of the $C_2H_3^{\bullet}$ and $C_4H_3^{\bullet}$ radicals to this reaction.

Because soot particles are formed from polycyclic aromatic hydrocarbons within the boundary layer at high temperatures in accordance with the aromaticity theory [23, 24], it seems necessary to estimate the possible contribution of these components to carbon film growth. The schemes of gas-phase reactions resulting in the formation of polyaromatic compounds [23, 24] include a great number of chemical components. This fact complicates solving set (1) of equations for the boundary layer. The upper estimate of the contribution of polycyclic aromatic hydrocarbons to the heterogeneous growth of the carbon film can reliably be obtained as follows. Neglecting the surface reaction, the boundary layer can approximately be considered as a chemical ideal plug-flow reactor with a temperature equal to the surface temperature and with a residence time of the gaseous mixture in it equal to $\tau \sim \delta^2/D$ (where D is the diffusion coefficient). The τ value is ~0.25 ms at a boundary layer thickness of 0.037 cm. By solving the spatially homogeneous non-steady-state system of equations $\partial a_i/\partial t = r_i$, where the a_i and r_i values are determined in set (1) of the equations, one can estimate the concentrations of chemical components in such a reactor at $t = \tau$. Figure 4 presents the solutions to the spatially homogeneous model for various temperatures and two residence times of the gaseous mixture in the reactor: 0.25 and 0.50 ms. In the spatially homogeneous model, the chemical scheme of the gas-phase reactions was substantially extended and contained the formation of benzene and naphthalene. For comparison, Fig. 4 also presents the vinylacetylene concentrations near the hot surface calculated according to set (1) of the equations for the boundary layer. As can be seen, the maximum vinylacetylene concentration in the spatially homogeneous model for 0.5 ms at 1400–2000 K is close to that calculated by the equations for transfer near the hot surface in the same temperature range. Taking into account a similar temperature dependence for the concentrations of vinylacetylene, benzene, and naphthalene (Fig. 4), one can obtain rough upper estimates for the concentrations of aromatic components near the surface heated to a temperature higher than 1400 K: $(2–5) \times 10^{-5}$ and $(1–2) \times 10^{-7}$ mole fraction for benzene and naphthalene, respectively. The concentrations of the higher polycyclic aromatic hydrocarbons in the boundary layer are still lower. Therefore, the contribution of polycyclic aromatic hydrocarbons to pyrocarbon formation in the experiments of [4, 5] remains negligibly small as compared to that of acetylene over the entire experimental temperature range. This is due to a short characteristic time of boundary layer “ventilation” and the slow accumulation of polycyclic aromatic hydrocarbons. Note that, near the surface with a temperature of more than 1600 K, further heating only causes an increase in the concentrations of polyines and their radicals (Fig. 3). The concentrations of all other gaseous products of acetylene pyrolysis decrease.

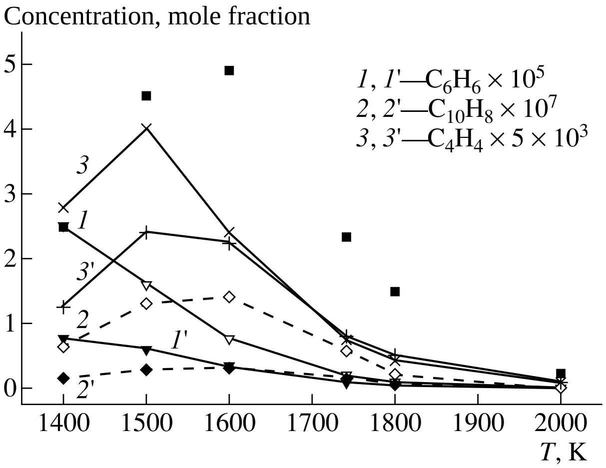

Fig. 4. Temperature dependence of the concentrations of (*1*, *1*') benzene, (*2*, *2*') naphthalene, and (*3*, *3*') vinylacetylene calculated from the kinetic equations under spatially homogeneous conditions at constant temperature. Curves (*1*, *2*, *3*) were calculated for the residence time in the reactor of 0.5 ms, whereas curves (*1*', *2*', *3*') correspond to the residence time of 0.25 ms. Filled squares represent the solution to set (1) of equations for the boundary layer for vinylacetylene.

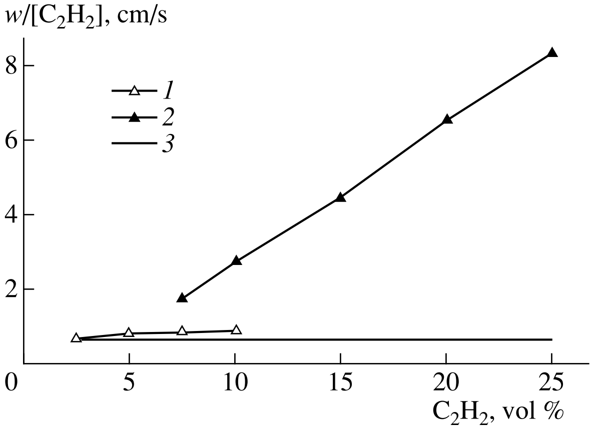

Fig. 5. Calculated curve for the reduced rate of carbon film formation $w/[C_2H_2]$ vs. acetylene concentration. T = 2000 K, δ = 0.037 cm: (*1*) the reduced rate of pyrocarbon formation; (*2*) the reduced rate of coke formation; and (*3*) the rate constant K for pyrocarbon formation from [5].

Al’tshuler [4, 5] claimed without sufficient experimental evidence that the heterogeneous pyrolysis is first-order with respect to acetylene concentration over the temperature range studied. Figure 5 presents the calculated reduced rate of coke and pyrocarbon formation as a function of acetylene concentration. Both the temperature (2000 K) and the boundary layer thickness (δ = 0.037 cm) remained unchanged. The curves in Fig. 5 suggest that the reduced rate of carbon film formation during polymerization is linearly proportional to the acetylene concentration; that is, the rate itself is proportional to the concentration to the second power. Under the conditions of pyrocarbon formation, the calculated reduced rate only slightly increases with an increase in the acetylene concentration because of an increase in the contribution of the products of bulk pyrolysis in the boundary layer. Figure 5 also shows that the mechanism of carbon film formation changes at an acetylene concentration of ~7% vol %.

The experimental data of [5] suggest that the rate of carbon film formation increases with a decrease in the rate of the approaching gas flow. Figure 6 compares the calculated and experimental [5] curves of the reduced rate vs. the gas flow rate. In both cases, the acetylene con-

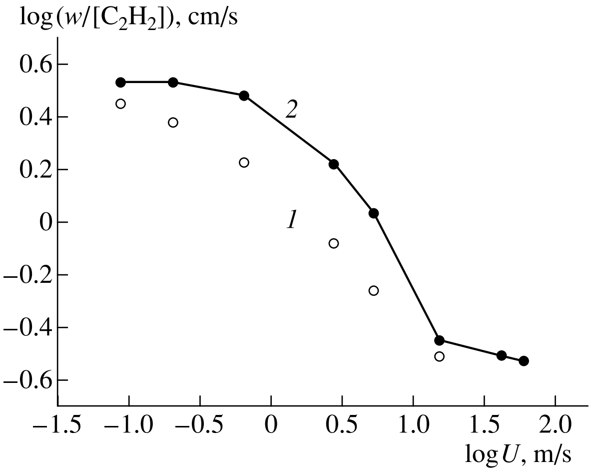

Fig. 6. Reduced rate of carbon film formation $w/[C_2H_2]$ as a function of the rate of the approach gas flow U: (*1*) the experimental value from [5] and (*2*) the calculated value.

centration (20% C_2H_2/Ar) and temperature (1773 K) coincide. The boundary layer thickness for different gas flow rates (U) was calculated by the equation $\delta = \delta_0\ (U_0/U)^{0.5} = 0.022$ cm, and $U_0 = 1.5 \times 10^3$ cm/s.

CONCLUSIONS

Comparison of the calculated and experimental data allows me to draw the following conclusions:

(a) The heterogeneous reaction on the surface of a solid (particle) cannot quantitatively be described within the framework of the model of pyrocarbon formation from gaseous hydrocarbons taking into account the contribution of the products of the gas-phase pyrolysis of acetylene. Under certain conditions (the acetylene concentration, the blowing rate, and temperature), the experimental rate of carbon film growth is much higher than that of pyrocarbon formation in this atmosphere.

(b) The gas-phase pyrolysis in the boundary layer an acetylene is passed around the hot surface forms the composition of atmosphere near the surface similar to that surrounding the soot particles during their nucleation. Therefore, the high rate of carbon film formation on the surface of a soot particle is solely determined by the properties of the hydrocarbon atmosphere surrounding this particle rather than the specific features of a new soot particles;

(c) The kinetics of the carbon film growth on the surface that accounts for the contribution of the products of the gas-phase pyrolysis of acetylene can quantitatively be described to a first approximation in terms of the approach developed earlier and applied to the growth of soot particles. However, the chemical mechanism that reflects an increase in the rate of the heterogeneous reaction under these conditions requires further extensive investigation.

REFERENCES

1. Tesner, P.A., *Kinetika obrazovaniya pirougleroda* (Kinetics of Pyrocarbon Formation), Moscow: VINITI, 1987.
2. Borodina, L.M. and Tesner, P.A., *Khim. Tverd. Topl.*, 1978, no. 6, p. 140.
3. Borodina, L.M. and Tesner, P.A., *Khim. Tverd. Topl.*, 1983, no. 4, p. 157.
4. Al’tshuler, B.N., *Kinet. Katal.*, 1974, vol. 15, no. 4, p. 835.
5. Al’tshuler, B.N., *Khim. Tverd. Topl.*, 1973, no. 4, p. 111.
6. Kiefer, J.H. and von Drasek, W.A., *Int. J. Chem. Kinet.*, 1990, vol. 22, p. 747.
7. Tesner, P.A., *Combust. Sci. Technol.*, 1994, vol. 97, p. 243.
8. Krestinin, A.V., *Khim. Fiz.*, 1994, vol. 13, no. 1, p. 121.
9. Krestinin, A.V., *Advanced Computation and Analysis of Combustion*, Roy, G.D., Frolov, S.M., and Givi, P., Eds., Moscow: ENAS, 1997, p. 38.
10. Krestinin, A.V., *Khim. Fiz.*, 1998, vol. 17, no. 8, p. 41.
11. Krestinin, A.V., *27th Symp. (Int.) on Combustion*, Pittsburgh: The Combustion Institute, 1998, p. 1557.
12. Krestinin, A.V., *Combust. Flame*, 2000, vol. 120, p. 513.
13. Schlichting, H., *Grenzschicht-Theorie*, Karlsrue: Verlag G. Braun, 1970.
14. Haynes, B.S. and Wagner, H.Gg., *Prog. Energy Combust. Sci.*, 1981, vol. 7, p. 229.
15. Minutolo, P., Gambi, G., D’Alessio, A., and D’Anna, A., *Combust. Sci. Technol.*, 1994, vol. 101, p. 311.
16. Howard, J.B., *23rd Symp. (Int.) on Combustion*, Pittsburgh: The Combustion Institute, 1990, p. 1107.
17. Dobbins, R.A., Govatzidakis, G.J., Lu, W., *et al.*, *Combust. Sci. Technol.*, 1996, vol. 121, p. 103.
18. Krestinin, A.V., Kislov, M.B., Raevskii, A.V., *et al.*, *Kinet. Katal.*, 2000, vol. 41, no. 1, p. 102.
19. Sukhinin, G.I. and Nerushev, O.A., *Prikl. Mekh. Tekh. Fiz.*, 1997, vol. 38, no. 4, p. 140.
20. Von Helden, G., Hsu, M.-T., Kemper, P.S., and Bowers, M.T., *J. Phys. Chem.*, 1991, vol. 95, p. 3835.
21. Kiefer, J.H., Mizerka, L.J., Patel, M.R., and Wei, H.-C., *J. Phys. Chem.*, 1985, vol. 89, p. 2013.
22. Fahr, A. and Stein, S.E., *22nd Symp. (Int.) on Combustion*, Pittsburgh: The Combustion Institute, 1988, p. 1023.
23. Frenklach, M., Clary, D.W., Gardiner, W.C., Jr., and Stein, S.E., *20th Symp. (Int.) on Combustion*, Pittsburgh: The Combustion Institute, 1984, p. 887.
24. Frenklach, M., Glary, D.W., Yuan, T., *et al.*, *Combust. Sci. Technol.*, 1986, vol. 50, p. 79.